Thermochimica Acta 527 (2012) 59–66

Contents lists available at SciVerse ScienceDirect

Thermochimica Acta

journal homepage: www.elsevier.com/locate/tca

Densities of ammonium and phosphonium based deep eutectic solvents: Prediction using artificial intelligence and group contribution techniques

K. Shahbaz[a], S. Baroutian[b], F.S. Mjalli[c,*], M.A. Hashim[a], I.M. AlNashef[d]

[a] Department of Chemical Engineering, University of Malaya, 50603 Kuala Lumpur, Malaysia
[b] SCION, Te Papa Tipu Innovation Park, 49 Sala Street, Private Bag 3020, Rotorua 3046, New Zealand
[c] Petroleum and Chemical Engineering Department, Sultan Qaboos University, 123 Muscat, Oman
[d] Department of Chemical Engineering, King Saud University, 11421 Riyadh, Saudi Arabia

ARTICLE INFO

Article history:
Received 18 August 2011
Received in revised form 4 October 2011
Accepted 5 October 2011
Available online 12 October 2011

Keywords:
Density
Deep eutectic solvent
Artificial neural network
Estimation

ABSTRACT

As applications of deep eutectic solvents are growing fast as green alternatives, prediction of physical properties data for such systems becomes a necessity for engineering application designs and new process developments. In this study, densities of three classes of deep eutectic solvents, based on a phosphonium and two ammonium salts, were measured. Two predictive models based on artificial intelligence and group contribution methods were proposed for accurate estimation and evaluation of deep eutectic solvent densities. A feed forward back propagation neural network with 9 hidden neurons was successfully developed and trained with the measured density data. The group contribution method applied the modified Lydersen–Joback–Reid, Lee–Kesler and the modified Rackett equations. The comparison of the predicted densities with those obtained by measurement confirmed the reliability of the neural network and the group contribution method with average absolute errors of 0.14 and 2.03%, respectively. Comparison of the model performances indicated a better predictability of the developed neural network over the group contribution method.

1. Introduction

Deep eutectic solvents (DESs) are gaining increasing attention in research and industry because of their potential as environmentally benign solvents and advantages over traditional ionic liquids such as non-toxicity, non-reactivity with water and most importantly being biodegradable [1]. In addition, they are prepared easily in high purity at low cost. One of the interesting features of using DESs is their potential as tunable solvents that can be customized to a particular type of chemistry [2]. DESs are created by mixing two or more components and they have low melting point compared to their constituting compounds. In other words, DESs are created from mixtures of an organic halide salt and an organic compound which is a hydrogen bond donor (HBD) able to form a hydrogen bond with the halide ion [3].

In spite of the importance of DESs and their interesting advantages, accurate values for many of their fundamental physical and chemical properties are either rare or even absent. The density is one of the important physical properties for DESs. DES density data play a key role in engineering application designs of this environmental friendly solvent. However, it is not practical to experimentally evaluate density in many cases. Therefore a great need arises for developing estimation methods of acceptable accuracy to fulfill this requirement [4].

Artificial neural networks (ANNs) is an estimation method which has been used widely for property predictions. ANNs are inspired and motivated by the structure and functional characteristics of human neurons and biological neural networks. Similar to the human nervous system, ANNs consists of an interrelated set of artificial neurons, and it processes information using a connectionist approach to computation. ANNs are computing systems, which can be trained to learn a complex relationship between two or more variables or data sets [5]. The ANNs are good for tasks involving incomplete data sets, fuzzy or incomplete information, and for highly complex and ill-defined problems, where humans usually decide on an intuitional basis [6]. Among the available artificial neural networks, the feed-forward neural network is one of the most important historical developments in neurocomputing [5]. Feed-forward neural network performs a weighted sum of its inputs and calculates an output using certain mathematical activation function embedded in its neurons.

ANNs have been used in number of fields of engineering, environmental sciences, mathematics and economics [6–9]. The application of ANNs in prediction physical and chemical properties of materials is increasing rapidly. Many studies have been carried out to predict densities of various materials using ANNs [10–18]. It

* Corresponding author. Tel.: +968 24142558; fax: +968 24141354.
E-mail address: farouqsm@yahoo.com (F.S. Mjalli).

0040-6031/$ – see front matter © 2011 Elsevier B.V. All rights reserved.
doi:10.1016/j.tca.2011.10.010

Table 1
Synthesized DESs compositions and freezing points.

Salt	HDB	x_{salt}	x_{HBD}	Abbreviation	Freezing temp. (K)
Choline chloride	Glycerol	0.50	0.50	DES1	281.18
	Glycerol	0.33	0.67	DES2	237.00
	Glycerol	0.25	0.75	DES3	240.50
	Ethylene glycol	0.36	0.64	DES4	239.83
	Ethylene glycol	0.33	0.67	DES5	207.14
	Ethylene glycol	0.28	0.72	DES6	277.30
N,N diethylenethanol ammonium chloride	Glycerol	0.33	0.67	DES7	271.82
	Glycerol	0.25	0.75	DES8	274.85
	Glycerol	0.20	0.80	DES9	275.12
	Ethylene glycol	0.33	0.67	DES10	242.15
	Ethylene glycol	0.25	0.75	DES11	250.90
	Ethylene glycol	0.20	0.80	DES12	251.48
Methyltriphenylphosphonium bromide	Glycerol	0.33	0.67	DES13	276.90
	Glycerol	0.25	0.75	DES14	267.60
	Glycerol	0.20	0.80	DES15	288.90
	Ethylene glycol	0.25	0.75	DES16	226.90
	Ethylene glycol	0.20	0.80	DES17	223.80
	Ethylene glycol	0.16	0.84	DES18	224.60

is proven that ANNs is a powerful data infilling technique to predict densities of liquids and gases.

Another technique, which has been widely used to predict density of liquids and gases with reasonable accuracy is the thermodynamic approach. For ionic liquids, thermodynamic approaches have been reported which are based on the corresponding state principle [19,20] and group contribution [21–23]. Unfortunately these methods suffer from high prediction errors because of the special ionic nature of ionic liquids and DESs. Recently, the authors have developed empirical group contribution method to predict densities of DESs [4]. In that technique the critical properties of salt and HBD were estimated separately using the modified Lydersen–Joback–Reid, Lee–Kesler method, while that of the mixture were calculated using Lee–Kesler equation. The Rackett equation modified by Spencer and Danner was employed to predict the DES density.

The purpose of this study is to measure and predict densities of three classes of deep eutectic solvents based on a phosphonium and two ammonium salts. An artificial neural network model was developed and trained using measured density data. The present work, applied a three layer back propagation neural network with 9 neurons in the hidden layer. The predicted densities by means of ANNs were compared with the results of the empirical group contribution method.

2. Methodology

2.1. DESs synthesis

In this work, 12 DESs based on ammonium salt and 6 DESs based on phosphonium salt were synthesized. Choline chloride ($C_5H_{14}ClNO$), N,N diethylenethanol ammonium chloride ($C_6H_{16}ClNO$) and methyl triphenyl phosphonium bromide ($C_{19}H_{18}PBr$) as salts and glycerol ($C_3H_8O_3$) and ethylene glycol ($C_2H_6O_2$) as hydrogen bond donors were purchased from Merck Chemicals and utilized for the synthesis of DESs without further purification. Synthesize of DESs were carried out using the method described earlier [4]. Table 1 presents the compositions and freezing temperature of the different DESs synthesized in this study (termed in this study as DES1–DES18). The freezing point measurements of all DESs were made using Mettler Toledo Differential Scanning Calorimeter which was calibrated against known standards to ensure the measurements accuracy. As indicated by Table 1, all the synthesized DESs gave low freezing points as contrasted to their constituting components. This is fitting with the general behavior of deep eutectic solvents. Furthermore, water content of all DESs was determined by Karl Fisher titration method and was found to be less than 0.1 wt% which was consistent with the physical properties of deep eutectic solvents.

2.2. Density measurement

Densities of the synthesized DESs were determined using a DMA 4500 vibrating tube density/specific gravity meter (Anton Paar, Austria). To check the density meter adjustment, density of water (degassed bi-distillated) was measured at 298.15 K. Comparison with the corresponding value in the density tables [24] showed a difference of $\pm 0.00003\ g\,cm^{-3}$ which confirmed the accuracy of machine. Density measurements were carried out at temperatures from 298.15 to 368.15 K at 5 K intervals with three replicates for each reading, the uncertainty in density measurements was $\pm 0.0001\ g\,cm^{-3}$.

2.3. Density prediction using neural network modeling

The methodology of the approach used in this study was accomplished through the implementation of the MATLAB neural networks toolbox [25]. In order to train and validate the neural network, measured densities of deep eutectic solvents were used. To enhance the training process and to increase the model accuracy the measured density data from our previous work were employed [4]. Tables 2–4 present the data sets for the three types of DESs. As can be seen the input parameters to the developed network include mole fractions of choline chloride ($x_{C_5H_{14}ClNO}$), N,N diethylenethanol ammonium chloride ($x_{C_6H_{16}ClNO}$) and methyl triphenyl phosphonium bromide ($x_{C_{19}H_{18}PBr}$) as sources of salt, mole fractions of glycerol ($x_{C_3H_8O_3}$) and ethylene glycol ($xC_2H_6O_2$) as hydrogen bond donors and temperature (K). The dataset was divided randomly into training and evaluation (60%) and simulation (40%). The training, validation and simulation data sets were consisted of the experimental data at (298.15, 313.15, 328.15, 343.15 and 358.15 K), (303.15, 318.15, 333.15, 343.15 and 363.15 K) and (308.15, 323.15, 338.15, 353.15 and 368.15 K), respectively.

This study, applied a feed-forward back propagation neural networks with hyperbolic tangent sigmoidal activation functions in three layers. The input, hidden and output layers had 6, 9 and 1 neurons, respectively, as shown in Fig. 1.

During the network training, the maximum number of epochs was set to 1000 and an early stopping criterion was adopted in order

Table 2
Density data set for choline chloride-based DESs.

Temp. (K)	Density (g cm^{-3})					
	DES1	DES2	DES3	DES4	DES5	DES6
298.15	1.1558[a]	1.1920	1.2030	1.1180	1.1174[a]	1.1170
303.15	1.1535	1.1895	1.2002	1.1156	1.1146	1.1141
308.15	1.1506[a]	1.1867	1.1976	1.1122	1.1117[a]	1.1111
313.15	1.1483	1.1838	1.1951	1.1097	1.1088	1.1082
318.15	1.1454[a]	1.1814	1.1922	1.1064	1.1059[a]	1.1052
323.15	1.1430	1.1776	1.1891	1.1037	1.1036	1.1023
328.15	1.1402[a]	1.1761	1.1868	1.1006	1.1001[a]	1.0993
333.15	1.1379	1.1741	1.1844	1.0968	1.0974	1.0962
338.15	1.1349[a]	1.1708	1.1814	1.0948	1.0944[a]	1.0934
343.15	1.1326	1.1674	1.1781	1.0910	1.0916	1.0904
348.15	1.1296[a]	1.1655	1.176	1.089	1.0885[a]	1.0875
353.15	1.1266	1.1635	1.1732	1.0870	1.0854	1.0847
358.15	1.1243[a]	1.1602	1.1706	1.0832	1.0826[a]	1.0816
363.15	1.1220	1.1571	1.1678	1.0820	1.0791	1.0788
368.15	1.1191[a]	1.1549	1.1652	1.0774	1.0767[a]	1.0757

[a] Ref. [4].

Table 3
Density data set for N,N-diethylenethanol ammonium chloride-based DESs.

Temp. (K)	Density (g cm^{-3})					
	DES7	DES8	DES9	DES10	DES11	DES12
298.15	1.1731[a]	1.2051	1.2201	1.0995	1.1018[a]	1.1037
303.15	1.1700	1.2020	1.2173	1.0965	1.0986	1.1004
308.15	1.1671[a]	1.1990	1.2141	1.0933	1.0955[a]	1.0973
313.15	1.1638	1.1961	1.2114	1.0903	1.0926	1.0942
318.15	1.1613[a]	1.1929	1.2081	1.0871	1.0893[a]	1.0910
323.15	1.1585	1.1884	1.2048	1.0840	1.0862	1.0877
328.15	1.1554[a]	1.1868	1.2021	1.0809	1.0830[a]	1.0846
333.15	1.1531	1.1840	1.1989	1.0778	1.0797	1.0815
338.15	1.1492[a]	1.1807	1.1961	1.0748	1.0767[a]	1.0782
343.15	1.1458	1.1777	1.1936	1.0717	1.0740	1.0750
348.15	1.1431[a]	1.1746	1.1901	1.0686	1.0705[a]	1.0718
353.15	1.1403	1.1719	1.1873	1.0655	1.0675	1.0683
358.15	1.1374[a]	1.1685	1.1841	1.0624	1.0642[a]	1.0654
363.15	1.1344	1.1661	1.1807	1.0590	1.0600	1.0622
368.15	1.1311[a]	1.1624	1.1781	1.0562	1.0546[a]	1.0590

[a] Ref. [4].

to avoid probable overfitting. The sigmoidal functions are often used in neural networks to introduce nonlinearity in the model and/or to make sure that certain signals remain within a specified range.

Selection of the number of neurons in the hidden layer is very important and this layer has a significant influence on the final output. Using too few neurons in the hidden layers will result in something called underfitting. On the other hand, too many neurons in this layer may result in overfitting and longer training time. For the selection of the neural network architecture, the optimum network architecture forward selection method was used [10]. A relatively small ANN structure was selected first. The network was trained and tested and its performance was tested in accordance with the experimental data.

Table 4
Density data set for methyl triphenyl phosphonium bromides-based DESs.

Temp. (K)	Density (g cm^{-3})					
	DES13	DES14	DES15	DES16	DES17	DES18
298.15	1.3064[a]	1.2976	1.2889	1.2501[a]	1.2326[a]	1.2195[a]
303.15	1.3030	1.2945	1.2855	1.2424	1.2290	1.2163
308.15	1.2990[a]	1.2906	1.2817	1.2432[a]	1.2256[a]	1.2124[a]
313.15	1.2952	1.2870	1.2780	1.2398	1.2220	1.2086
318.15	1.2920[a]	1.2836	1.2745	1.2363[a]	1.2185[a]	1.2052[a]
323.15	1.2886	1.2809	1.2710	1.2324	1.2151	1.2020
328.15	1.2851[a]	1.2766	1.2673	1.2293[a]	1.2114[a]	1.1980[a]
333.15	1.2817	1.2736	1.2634	1.2260	1.2079	1.1947
338.15	1.2782[a]	1.2696	1.2601	1.2223[a]	1.2043[a]	1.1907[a]
343.15	1.2749	1.2660	1.2568	1.2188	1.2006	1.1870
348.15	1.2715[a]	1.2626	1.2529	1.2153[a]	1.1972[a]	1.1834[a]
353.15	1.2682	1.2593	1.2495	1.2119	1.1936	1.1792
358.15	1.2648[a]	1.2556	1.2457	1.2083[a]	1.1900[a]	1.1761[a]
363.15	1.2615	1.2524	1.2423	1.2045	1.1864	1.1723
368.15	1.2581[a]	1.2486	1.2385	1.2013[a]	1.1828[a]	1.1688[a]

[a] Ref. [4].

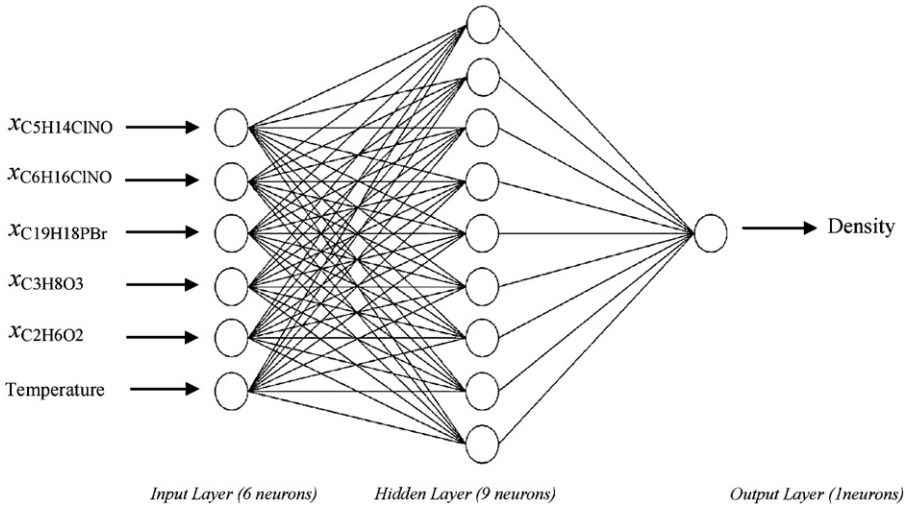

Fig. 1. Configuration on a 6–9–1 neural network for prediction of DESs density.

2.4. Density prediction using group contribution method

In this study, the modified Lydersen–Joback–Reid, Lee–Kesler method was selected as the method of choice for estimating the critical properties of salts and hydrogen bond donors separately. Calculation of critical properties and acentric factor of each component was carried out using the methods described previously [4].

The Lee–Kesler mixing rules equations recommended by Knapp et al. [27] were employed to calculate the critical properties of DESs [4]. Finally, The Rackett equation modified by Spencer and Danner [28] was employed to predict the DES densities at various temperatures. The density at 298.15 K for each DES was chosen as the reference density needed by the method to predict DESs densities at other different temperatures [4].

2.5. Statistical assessment of density predictions

In this work, to assess the developed neural networks and the group contribution method to know the extent to which they can be used with better prediction quality of the DESs densities, several statistical descriptors were calculated and their values compared [26]. These are the index of agreement (IA) showing the overall accuracy of the model, fractional bias (FB) measuring tendency of the model to over-prediction or under-prediction, normalized mean square error (NMSE) showing the overall accuracy of the model, geometric variance (VG) indicating systematic and random errors, geometric mean bias (MG) identifying systematic errors and regression coefficient (R^2) describing the association between measured densities and predicted results. The calculation expressions for these descriptors are given below:

$$\mathrm{IA} = 1 - \frac{\sum_{i=1}^{N}(P_i - E_i)^2}{\sum_{i=1}^{N}(|P_i - \bar{E}| + |O_i - \bar{E}|)^2} \quad (1)$$

$$\mathrm{FB} = \frac{\bar{E} - \bar{P}}{0.5(\bar{E} + \bar{P})} \quad (2)$$

$$\mathrm{NMSE} = \frac{\overline{(E - P)^2}}{\overline{E}\,\overline{P}} \quad (3)$$

$$\mathrm{MG} = \exp(\overline{\ln E} - \overline{\ln P}) \quad (4)$$

$$\mathrm{VG} = \exp\overline{[(\ln E - \ln P)^2]} \quad (5)$$

where E, P, $\bar{E}$ and $\bar{P}$ are measured density, predicted density, average of the entire experimental dataset and average of the entire prediction dataset, respectively.

3. Results and discussion

3.1. Density measurement

Eighteen DESs with various compositions were synthesized. The densities of all synthesized DESs were measured from 298.15 to 368.15 K at 5 K interval with an average uncertainty of $\pm 0.0001\ \mathrm{g\,cm^{-3}}$. Tables 2–4 present measured densities of the choline chloride-based DESs (DES1–DES6), N,N diethylenethanol ammonium chloride-based DESs (DES7–DES12) and methyl triphenyl phosphonium bromide-based DESs (DES13–DES18), respectively. The results indicate that the all synthesized DESs demonstrate temperature-dependent behavior; the liquid density of the all DESs decreased linearly with the increase in temperature.

3.2. Neural network modeling

As described before, a feed forward back propagation neural network of a three layers structure was selected. Different numbers of hidden neurons were tested and based on evaluation results it was found that the network with 9 hidden neurons has the best prediction performance. Fig. 2 shows the result of training evaluation for the network with 9 hidden neurons against the measured densities. As can be seen, the trained data are in very good agreement with the measured data. This indicates that the network has been well trained and can be used to predict DESs densities at a wide range of input conditions. The simulation result is shown in Fig. 3. A good agreement was observed between the measured densities and the predicted data. The linear correlation and the regression constants (R^2-value), in Figs. 2 and 3, confirm the agreements of trained and simulated data with the experimental data.

Table 5 compares measured densities (at 308.15, 323.15, 338.15, 353.15 and 368.15 K) with those predicted by ANNs in terms of absolute relative percentage error (ARPE). Although the measured DESs densities seem to be diverse, it is obvious that the ANN with a 9 hidden neurons based on the standard back-propagation algorithm, resulted as a very effective model to predict density. The absolute average error of this prediction was 0.14%, which is very good. The good predictability of ANNs can be attributed

Table 5
Absolute relative percentage error (ARPE) in the predicted DESs densities using ANNs method (method 1) and group contribution method (method 2).

Abbreviation	Method	Temperature (K)				
		308.15	323.15	338.15	353.15	368.15
DES1	1	0.209	0.201	0.159	0.115	0.223
	2	0.579	1.493	2.402	3.332	4.373
DES2	1	0.194	0.051	0.188	0.266	0.199
	2	0.566	1.345	2.351	3.352	4.283
DES3	1	0.184	0.126	0.178	0.247	0.197
	2	0.550	1.368	2.285	3.196	4.161
DES4	1	0.189	0.154	0.128	0.340	0.195
	2	0.654	1.691	2.747	3.956	5.070
DES5	1	0.228	0.272	0.174	0.221	0.176
	2	0.665	1.739	2.770	3.877	5.075
DES6	1	0.144	0.200	0.128	0.157	0.139
	2	0.650	1.670	2.734	3.876	5.053
DES7	1	0.146	0.216	0.113	0.132	0.283
	2	0.482	1.265	2.022	2.848	3.687
DES8	1	0.125	0.034	0.127	0.137	0.138
	2	0.485	1.118	2.025	2.874	3.703
DES9	1	0.091	0.100	0.125	0.067	0.144
	2	0.497	1.243	2.070	2.931	3.779
DES10	1	0.166	0.101	0.181	0.235	0.087
	2	0.587	1.504	2.477	3.505	4.589
DES11	1	0.168	0.101	0.123	0.206	0.351
	2	0.596	1.532	2.507	3.562	4.347
DES12	1	0.094	0.064	0.104	0.112	0.052
	2	0.595	1.517	2.505	3.511	4.632
DES13	1	0.077	0.427	0.477	0.237	0.064
	2	0.152	0.446	0.756	1.114	1.482
DES14	1	0.015	0.086	0.150	0.151	0.296
	2	0.229	0.650	0.966	1.378	1.780
DES15	1	0.023	0.064	0.016	0.136	0.024
	2	0.243	0.633	1.024	1.461	1.890
DES16	1	0.047	0.017	0.057	0.116	0.047
	2	0.320	0.770	1.307	1.851	2.407
DES17	1	0.046	0.041	0.021	0.075	0.040
	2	0.345	0.893	1.441	2.038	2.658
DES18	1	0.039	0.092	0.068	0.051	0.024
	2	0.369	0.973	1.540	2.118	2.829

to its adaptability that changes its structure based on external or internal information that flows through the network during the learning phase [29]. In this work because of the adequate amount of training data, the network trained well and the outputs were precise. Table 5 also shows that the ANNs has the highest prediction accuracy for the methyl triphenyl phosphonium bromide:ethylene glycol DESs (DES16–DES18) and N,N diethylenethanol ammonium chloride:glycerol DESs (DES7 and DES8) with average ARPE of 0.05 and 0.13%, respectively.

3.3. Group contribution method

In this work a thermodynamic model was proposed to predict densities of all synthesized DESs (at 308.15, 323.15, 338.15, 353.15 and 368.15 K). As described before, the model used the group contributions, mixing rules equations and the modified Rackett equation for estimating the critical properties of component, DES critical properties and density, respectively.

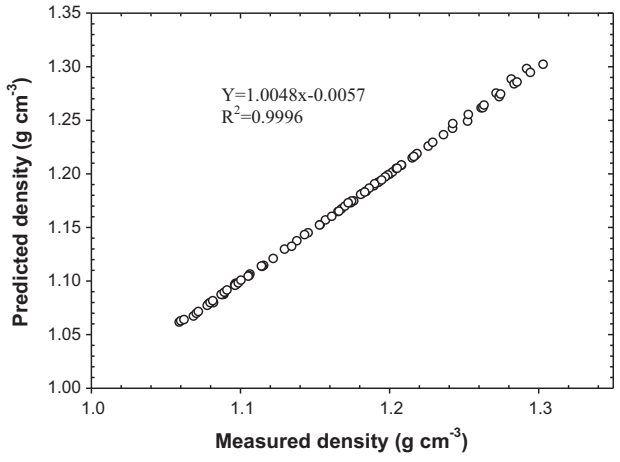

Fig. 2. Validation result for the network with 9 hidden neurons.

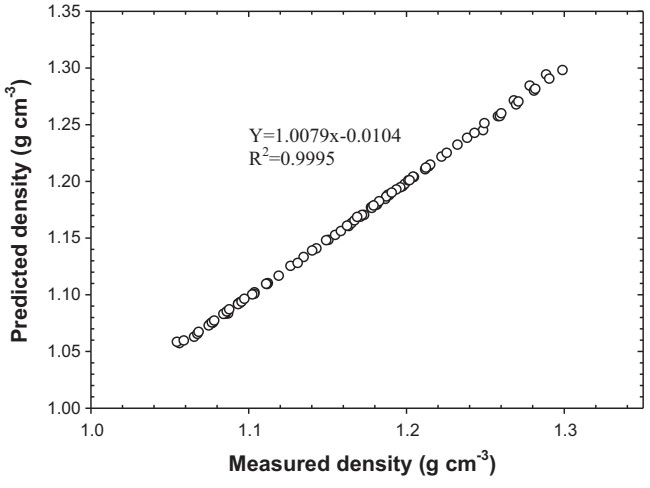

Fig. 3. Comparison between simulation results using 9 neurons in the hidden layer and measured DESs densities.

Table 6
Statistical assessment of the potential of using ANNs method (method 1) and group contribution method (method 2).

Method	R^2 (1.000) [a]	IA (1.000) [a]	FB (0.000) [a]	NMSE (0.000000) [a]	MG (1.00000) [a]	VG (1.00000) [a]	ARPE (0.000) [a]
1	0.9995	0.99979	0.00099	0.000002	1.00102	1.00000	0.142
2	0.9748	0.96512	0.20054	0.000550	1.20843	1.00061	2.032

[a] Numbers in brackets are ideal values.

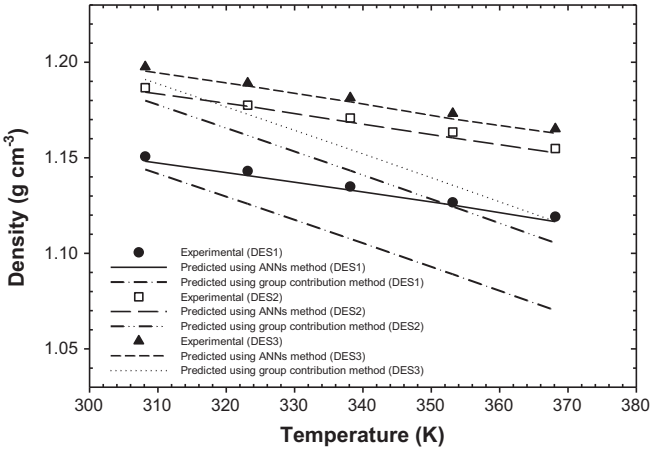

Fig. 4. Experimental and predicted densities of choline chloride:glycerol DESs.

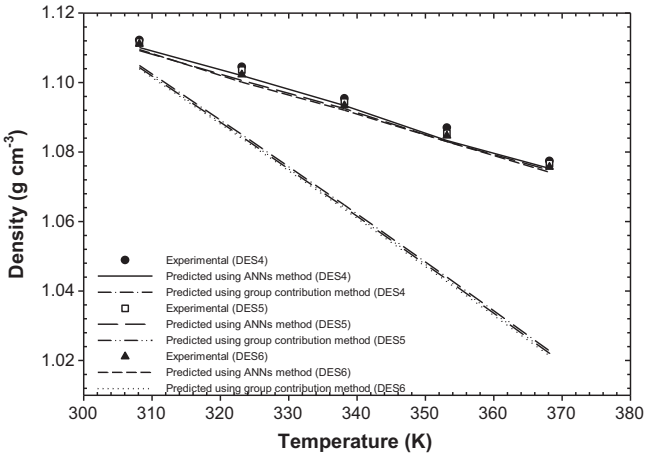

Fig. 5. Experimental and predicted densities of choline chloride:ethylene glycol DESs.

The prediction results from the group contribution method were compared with those obtained experimentally. Table 5 shows this comparison by means of ARPE. The average ARPE of this prediction was 2.03%, which is reasonably good. Table 6 reveals that the group contribution method has the highest prediction accuracy for the methyl triphenyl phosphonium bromide:ethylene glycol DESs (DES16–DES18) and methyl triphenyl phosphonium bromide:glycerol DESs (DES13–DES15). The average ARPE for these two phosphonium-based DESs were 0.95 and 1.46%, respectively.

3.4. Statistical assessment

The results of statistical assessment are summarized in Table 6. The prediction accuracy of the 9 hidden neurons network was superior to the group contribution method. The overall agreement between modeled and measured values for the ANNs and group contribution method varied considerably (IA = 0.96512–0.99979 and R^2 = 0.9748–0.9995). A highest agreement achieved for ANNs while the group contribution model was in a reasonable agreement.

The model bias appeared to be significantly low overestimation for the neural network with 9 hidden neurons. Comparison indicates that overestimation for the group contribution method was not low as ANNs but its bias was in a satisfactory range.

Also, the highest overall accuracy in terms of normalized mean square error (NMSE) was achieved for ANNs model (2.8×10^{-6}). A non-significant normalized mean square error for the group contribution method (5.5×10^{-4}) confirms reasonable accuracy of this model. The values of geometric variance (VG) and geometric mean bias (MG) revealed that both models were successful to predict density in terms of systematic and random errors.

3.5. Influences of temperature and composition

The predicted results from the developed ANNs and the group contribution method were used to investigate the effect of temperature and composition on the density of DESs. Figs. 4–9 show the predicted densities using ANNs and group contribution method along with the experimental data and indicate that DESs densities decrease linearly with increase in temperature. It is obvious that

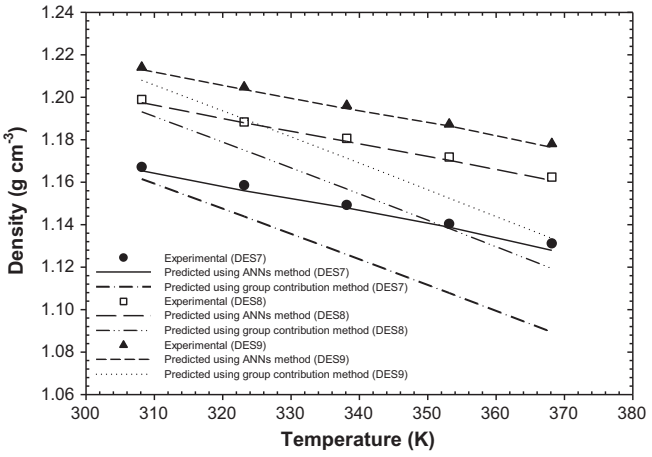

Fig. 6. Experimental and predicted densities of N,N diethyl ethanol ammonium chloride:glycerol DESs.

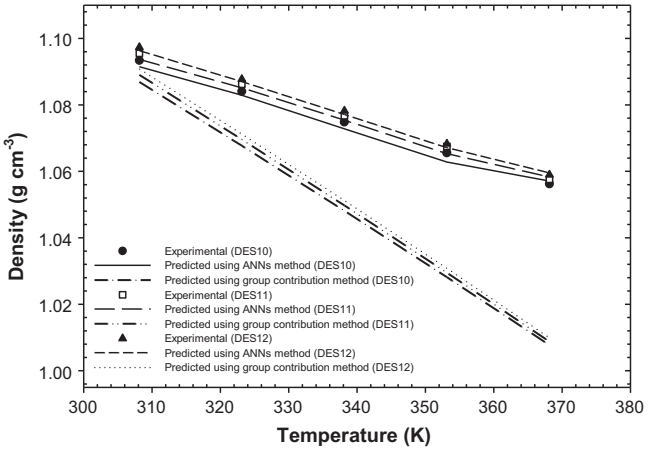

Fig. 7. Experimental and predicted densities of N,N diethyl ethanol ammonium chloride:ethylene glycol DESs.

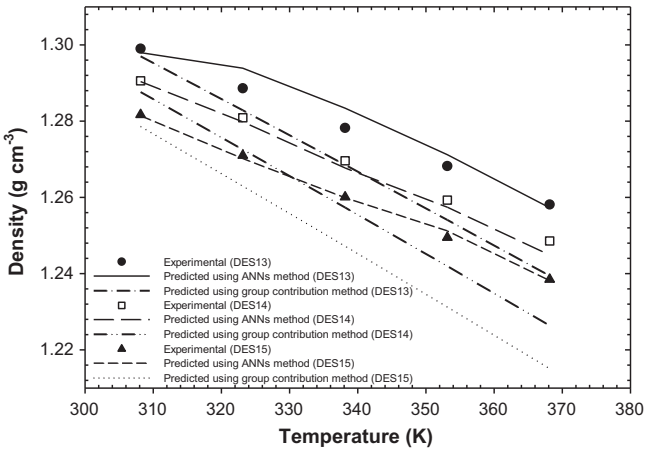

Fig. 8. Experimental and predicted densities of methyl triphenyl phosphonium bromide:glycerol DESs.

because of the greater molecular degree of motion at high temperatures, volume is expanded and thus the density is decreased.

It was found that the increase in the mole fraction of glycerol as HBD increased the densities of choline chloride-based DESs and N,N diethyl ethanol ammonium chloride-based DESs (Figs. 4 and 6). This is attributed to the fact that the glycerol density (1.2610 g cm^3) is higher than the density of the corresponding DESs. However, for the methyl triphenyl phosphonium bromide-based DESs, increase in the mole fraction of glycerol has a negative effect on the density because of the higher corresponding DESs densities (Fig. 8). With the same reasoning stated above, the results revealed that increase in the mole fractions of ethylene glycol as HBD increased the densities of N,N diethyl ethanol ammonium chloride-based DESs (Fig. 7) and decreased the densities of choline chloride-based DESs and methyl triphenyl phosphonium bromide-based DESs (Figs. 5 and 9).

The comparison of the performances of ANN and group contribution models at different temperatures shows that the ANN model has better predictabilities especially at higher temperatures (>323.15 K) for all the synthesized DESs. A possible reason for the lower accuracy of the group contribution method at higher temperatures can be attributed to sensitivity of saturated molar volume of liquid and compressibility factor to temperature.

The effect of DESs compositions on the performances of the predictive models indicates that the accuracy of the ANN model increased with increase in the hydrogen bond donor concentrations for all the synthesized DESs. For the choline chloride-based DESs (DES1–DES6) and N,N diethyl ethanol ammonium chloride-based DESs (DES7–DES12) increase in the hydrogen bond donor concentrations improved the predictability of group contribution model. On the other hand, the accuracy of the group contribution model was decreased with increase in the hydrogen bond donor contents of methyl triphenyl phosphonium bromide-based DESs (DES13–DES18). A possible reason can be the higher density of methyl triphenyl phosphonium bromide salt, which is too different from the other ammonium salts.

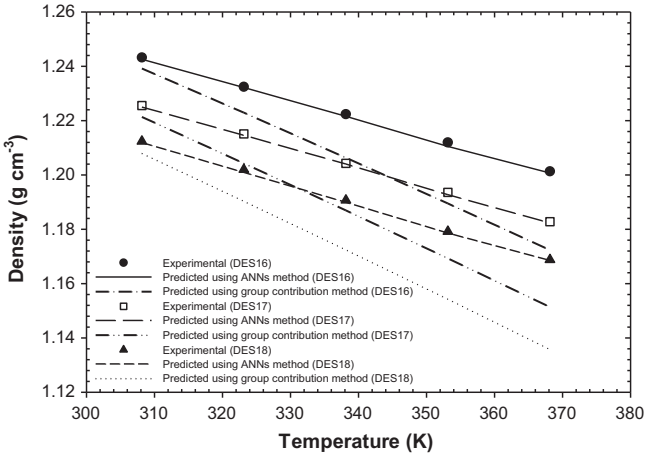

Fig. 9. Experimental and predicted densities of methyl triphenyl phosphonium bromide:ethylene glycol DESs.

4. Conclusion

In this work, densities of three types of deep eutectic solvents based on ammonium and phosphonium salts were determined at various temperatures and compositions. Temperature and composition were found to be of significant influence on the DES densities. Two methods of prediction, based on artificial intelligence and group contribution method were proposed for prediction of DESs densities. The comparison of the predicted densities with those obtained by measurement confirmed the reliability of the ANN and the group contribution method with average ARPE of 0.14 and 2.03%, respectively. It was found that the ANN model is more accurate to predict densities of the DESs at different compositions and temperature. The advantage of neural based model for predicting DESs densities is more obvious at temperatures higher than 323.15 K.

Acknowledgments

The authors thank the Deanship of Scientific Research at King Saud University for funding the work through group project No. RGP-VPP-108. The authors express their appreciations to the Centre for Ionic Liquids (UMCiL), University of Malaya and to the Petroleum and Chemical Engineering Department, Sultan Qaboos University, for their support to this research project.

Appendix A. Supplementary data

Supplementary data associated with this article can be found, in the online version, at doi:10.1016/j.tca.2011.10.010.

References

[1] A.P. Abbott, D. Boothby, G. Capper, D.L. Davies, R.K. Rasheed, Deep eutectic solvents formed between choline chloride and carboxylic acids: versatile alternatives to ionic liquids, J. Am. Chem. Soc. 126 (2004) 9142–9147.
[2] C.A. Nkuku, R.J. LeSuer, Electrochemistry in deep eutectic solvents, J. Phys. Chem. B 111 (2007) 13271–13277.
[3] K. Shahbaz, F.S. Mjalli, M.A. Hashim, I.M. AlNashef, Using Deep eutectic solvents based on methyl triphenyl phosphunium bromide for the removal of glycerol from palm-oil-based biodiesel, Energy Fuels 25 (2011) 2671–2678.
[4] K. Shahbaz, F.S. Mjalli, M.A. Hashim, I.M. AlNashef, Prediction of deep eutectic solvents densities at different temperatures, Thermochim. Acta 515 (2011) 67–72.
[5] A. Mohebbi, S. Baroutian, Estimation of particle concentration emitted from the stacks of kerman cement plant using artificial neural networks, Chem. Eng. Commun. 195 (2008) 821–833.
[6] S.A. Kalogirou, Artificial neural networks in renewable energy systems applications: a review, Renew. Sustain. Energy Rev. 5 (2001) 373–401.
[7] F.S. Mjalli, A. Al-Mfargi, Neural network-based heat and mass transfer coefficients for the hybrid modeling of fluidized reactors, Chem. Eng. Commun. 197 (2009) 318–342.
[8] M. Satyanarayana, C. Muraleedharan, Prediction of acid values of vegetable oils having high free fatty acids using artificial neural networks, Energy Source A 32 (2010) 1479–1489.
[9] G. Lisa, D.A. Wilson, S. Curteanu, C. Lisa, C.-G. Piuleac, V. Bulacovschi, Ferrocene derivatives thermostability prediction using neural networks and genetic algorithms, Thermochim. Acta 521 (2011) 26–36.
[10] S. Baroutian, M.K. Aroua, A.A. Abdul Raman, N.M. Nik Sulaiman, Estimation of vegetable oil-based ethyl esters biodiesel densities using artificial neural networks, J. Appl. Sci. 8 (2008) 3005–3011.

[11] A.A. AlQuraishi, E.M. Shokir, Artificial neural networks modeling for hydrocarbon gas viscosity and density estimation, J. King Saud Univ. (Eng. Sci.) 23 (2011) 123–129.
[12] J.A. Lazzús, [rho]-T-P prediction for ionic liquids using neural networks, J. Taiwan Inst. Chem. Eng. 40 (2009) 213–232.
[13] A.R. Moghadassi, M.R. Nikkholgh, F. Parvizian, S.M. Hosseini, Estimation of thermophysical properties of dimethyl ether as a commercial refrigerant based on artificial neural networks, Expert. Syst. Appl. 37 (2010) 7755–7761.
[14] M. Mohebbi, A. Taheri, Soltani, A neural network for predicting saturated liquid density using genetic algorithm for pure and mixed refrigerants, Int. J. Refrig. 31 (2008) 1317–1327.
[15] M.S. Ozerdem, Artificial neural network approach to predict the electrical conductivity and density of Ag–Ni binary alloys, J. Mater. Process. Technol. 208 (2008) 470–476.
[16] A.A. Rohani, G. Pazuki, H.A. Najafabadi, S. Seyfi, M. Vossoughi, Comparison between the artificial neural network system and SAFT equation in obtaining vapor pressure and liquid density of pure alcohols, Expert. Syst. Appl. 38 (2011) 1738–1747.
[17] H. Yang, Z. Ring, Y. Briker, N. McLean, W. Friesen, C. Fairbridge, Neural network prediction of cetane number and density of diesel fuel from its chemical composition determined by LC and GC–MS, Fuel 81 (2002) 65–74.
[18] F. Gharagheizi, G.R. Salehi, Prediction of enthalpy of fusion of pure compounds using an artificial neural network-group contribution method, Thermochim. Acta 521 (2011) 37–40.
[19] J.O. Valderrama, W.W. Sanga, J.A. Lazzus, Critical Properties, Normal boiling temperature, and acentric factor of another 200 ionic liquids, Ind. Eng. Chem. Res. 47 (2008) 1318–1330.
[20] J.O. Valderrama, P.A. Robles, Critical Properties, Normal boiling temperatures, and acentric factors of fifty ionic liquids, Ind. Eng. Chem. Res. 46 (2007) 1338–1344.
[21] A.P. Coutinho Jo, L. Gardas Ramesh, Predictive group contribution models for the thermophysical properties of ionic liquids, in: Ionic Liquids: From Knowledge to Application, American Chemical Society, 2009, pp. 385–401.
[22] J. Jacquemin, R. Ge, P. Nancarrow, D.W. Rooney, M.F. Costa Gomes, A.A.H. Pàdua, C. Hardacre, Prediction of ionic liquid properties. I. Volumetric properties as a function of temperature at 0.1 MPa, J. Chem. Eng. Data 53 (2008) 2473.
[23] J.O. Valderrama, A. Reàtegui, R.E. Rojas, Density of ionic liquids using group contribution and artificial neural networks, Ind. Eng. Chem. Res. 48 (2009) 3254–3259.
[24] H. Bettin, F. Spieweck, Die Dichte des Wassers als Funktion der Temperatur nach Einführung der Internationalen Temperaturskala, PTB-Mitt. 1 (1990) 195–196.
[25] H. Demuth, M. Beale, Neural Network Toolbox for use with Matlab User Guide, The MathWorks Natick, MA, 2000.
[26] S. Hanna, E. Baja, A simple urban dispersion model tested with tracer data from Oklahoma City and Manhattan, Atmos. Environ. 43 (2009) 778–786.
[27] H. Knapp, R. Doring, L. Oellerich, U. Plocker, J.M. Prauznits, R. Langhorst, S. Zeck, Vapor–liquid equilibria for mixtures of low boiling substances, DECHEMA Chem. Data Series (1982).
[28] C.F. Spencer, R.P. Danner, Improved equation for prediction of saturated liquid density, J. Chem. Eng. Data 17 (1972) 236–241.
[29] S. Baroutian, M.K. Aroua, A.A.A. Raman, N.M.N. Sulaiman, Methanol recovery during transesterification of palm oil in a TiO_2/Al_2O_3 membrane reactor: experimental study and neural network modeling, Sep. Purif. Technol. 76 (2010) 58–63.